7978 *Biochemistry* **2010,** *49,* 7978–7987
DOI: 10.1021/bi101056m

BIOCHEMISTRY
including biophysical chemistry & molecular biology
Article

Stereoselective Hydrolysis of Organophosphate Nerve Agents by the Bacterial Phosphotriesterase[†]

Ping-Chuan Tsai,[‡] Andrew Bigley,[‡] Yingchun Li,[‡] Eman Ghanem,[‡] C. Linn Cadieux,[§] Shane A. Kasten,[§] Tony E. Reeves,[§] Douglas M. Cerasoli,[§] and Frank M. Raushel*[,‡]

[‡]*Department of Chemistry, P.O. Box 30012, Texas A&M University, College Station, Texas 77842, and* [§]*U.S. Army Medical Research Institute of Chemical Defense, 3100 Ricketts Point Road, Aberdeen Proving Ground, Maryland 21010-5400*

Received July 1, 2010; Revised Manuscript Received August 6, 2010

ABSTRACT: Organophosphorus compounds include many synthetic, neurotoxic substances that are commonly used as insecticides. The toxicity of these compounds is due to their ability to inhibit the enzyme acetylcholine esterase. Some of the most toxic organophosphates have been adapted for use as chemical warfare agents; the most well-known are GA, GB, GD, GF, VX, and VR. All of these compounds contain a chiral phosphorus center, with the S_P enantiomers being significantly more toxic than the R_P enantiomers. Phosphotriesterase (PTE) is an enzyme capable of detoxifying these agents, but the stereochemical preference of the wild-type enzyme is for the R_P enantiomers. A series of enantiomerically pure chiral nerve agent analogues containing the relevant phosphoryl centers found in GB, GD, GF, VX, and VR has been developed. Wild-type and mutant forms of PTE have been tested for their ability to hydrolyze this series of compounds. Mutant forms of PTE with significantly enhanced, as well as relaxed or reversed, stereoselectivity have been identified. A number of variants exhibited dramatically improved kinetic constants for the catalytic hydrolysis of the more toxic S_P enantiomers. Improvements of up to 3 orders of magnitude relative to the value of the wild-type enzyme were observed. Some of these mutants were tested against racemic mixtures of GB and GD. The kinetic constants obtained with the chiral nerve agent analogues accurately predict the improved activity and stereoselectivity against the authentic nerve agents used in this study.

Organophosphorus compounds have been utilized for more than 50 years as insecticides for the protection of agricultural crops (*1*), and similar compounds have been developed as chemical warfare agents (*2*). The structures of these latter compounds are presented in Scheme 1 and include tabun (GA), sarin (GB), soman (GD), cyclosarin (GF), VX, and VR. GA has a cyanide leaving group; the three remaining G agents (GB, GD, and GF) have a fluoride leaving group, and the two versions of VX have a thiolate leaving group. The toxicity of these organophosphonates is due to the inactivation of acetylcholinesterase (AChE),[1] an enzyme that catalyzes the hydrolysis of acetylcholine at neural synapses, through the phosphonylation of an active site serine residue (*3*). GA, GB, GF, VX, and VR contain a chiral phosphorus center, and thus, each of these nerve agents has two stereoisomers; soman has four stereoisomers because of an additional chiral center within the pinacolyl substituent. The enantiomers are differentially toxic; the S_P stereoisomer of sarin reacts with AChE approximately $\sim 10^4$ times faster than the R_P stereoisomer, and the two S_P stereoisomers of soman react $\sim 10^5$ times faster than the two R_P isomers. Similarly, the S_P stereoisomer of VX is ~100-fold more toxic than the R_P stereoisomer (*2*).

The detoxification of organophosphorus nerve agents can be catalyzed by organophosphate degrading enzymes such as human paraoxonase 1 (PON1), squid DFPase, organophosphorus acid anhydrolase (OPAA), and phosphotriesterase (PTE). Human paraoxonase is capable of hydrolyzing GB and GD, but the overall catalytic activity is relatively low (*4*). The DFPase from *Loligo vulgaris* is able to hydrolyze GA, GB, GD, GF, and DFP (diisopropyl fluorophosphate). The value of k_{cat}/K_m for the hydrolysis of DFP is $\sim 1.3 \times 10^6$ M^{-1} s^{-1}, but the catalytic activities for the hydrolysis of GB and GD are significantly lower (*5*, *6*). Organophosphorus acid anhydrolase from *Alteromonas* sp. JD6.5 is capable of hydrolyzing a wide variety of organophosphorus compounds, including GB, GD, and GF but not VX (*7*). Phosphotriesterase was first isolated from soil microbes (*8*). The best substrate identified to date for this enzyme is the agricultural pesticide paraoxon, and the value of k_{cat}/K_m approaches the diffusion-controlled limit of $\sim 10^8$ M^{-1} s^{-1} (*9*). The enzymatic reaction for the hydrolysis of paraoxon to *p*-nitrophenol and diethyl phosphate is shown in Scheme 2. The substrate specificity of PTE is quite broad, and this enzyme is capable of hydrolyzing GA, GB, GD, GF, VR, and VX (*10*).

PTE is a homodimeric protein that contains a binuclear metal center embedded within a $(\beta/\alpha)_8$-barrel structure and is a member of the amidohydrolase superfamily (*11*). The native enzyme contains two Zn^{2+} ions, and these metal ions can be substituted with Cd^{2+}, Co^{2+}, Ni^{2+}, or Mn^{2+} without a loss of catalytic activity (*9*). Previous investigations have identified three subsites within the active site of PTE that help to define the substrate specificity for this enzyme (*12*). The small pocket is defined by the

[†]This work was supported by National Institutes of Health Grant GM 68550.

*To whom correspondence should be addressed. Telephone: (979) 845-3373. Fax: (979) 845-9452. E-mail: raushel@tamu.edu.

[1]Abbreviations: PTE, phosphotriesterase; AChE, acetylcholine esterase; ITC, isothermal titration calorimetry; PON1, human paraoxonase 1; OPAA, organophosphorus acid anhydrolase; DFP, diisopropyl fluorophosphate.

 Published on Web 08/11/2010

Scheme 1: Structures of Chemical Warfare Agents

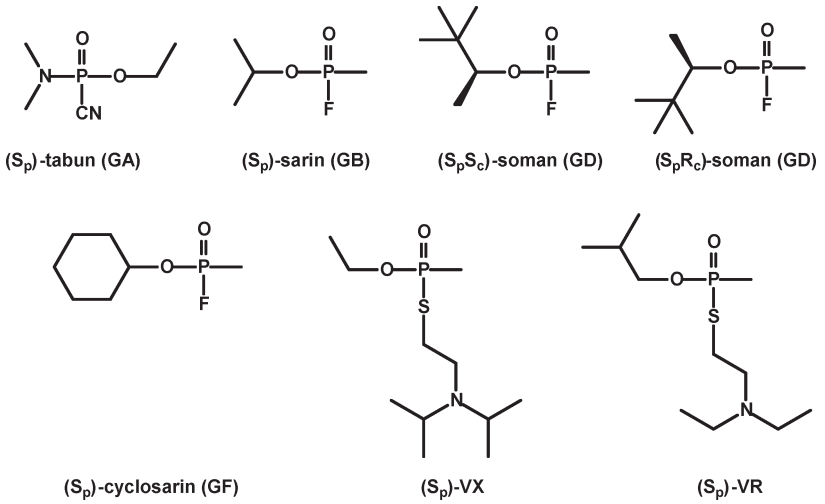

Scheme 2: Hydrolysis of Paraoxon by Phosphotriesterase

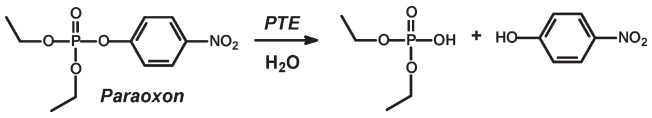

side chains of Gly-60, Ile-106, Leu-303, and Ser-308. The large pocket is formed by the interactions of His-254, His-257, Leu-271, and Met-317. The leaving group pocket is surrounded by four aromatic residues: Trp-131, Phe-132, Phe-306, and Tyr-309. The substrate binding site of PTE is graphically presented in Figure 1.

Wild-type PTE is stereoselective for the hydrolysis of chiral organophosphates (*13*), and the degree of stereoselectivity depends on the substituents attached to the central phosphorus core (*14*, *15*). For example, wild-type PTE hydrolyzes the R_P enantiomer of phenyl 4-acetylphenyl methylphosphonate approximately 2 orders of magnitude faster than the S_P enantiomer (*15*). The stereoselectivity of PTE can be manipulated through the mutation of residues that contact the substrate prior to catalytic turnover. Thus, the G60A mutant hydrolyzes the R_P enantiomer of phenyl 4-acetylphenyl methylphosphonate ~5 orders of magnitude faster than the S_P enantiomer (*15*). Unfortunately, the inherent stereoselectivity of wild-type PTE does not match that of AChE because PTE preferentially hydrolyzes the least toxic enantiomer of chiral organophosphates (*16*). However, the stereoselectivity of PTE can be inverted through multiple mutations to the small and large pockets in the active site (*15*). For example, the I106G/F132G/H257Y mutant catalyzes the hydrolysis of the S_P enantiomer of phenyl 4-acetylphenyl methylphosphonate ~3 orders of magnitude faster than the R_P enantiomer (*15*). This represents a change in stereoselectivity of nearly 8 orders of magnitude relative to that of the G60A mutant with only four amino acid changes.

In this paper, we describe the synthesis of chiral analogues of GB, GD, GF, VX, and VR with a 4-acetylphenol leaving group (Scheme 3). We have utilized these compounds to test a series of mutant forms of PTE that have been previously shown to have stereochemical preferences differing from those of the wild-type enzyme (*14*, *15*, *17*). This analysis has allowed the identification of variants enhanced in their ability to hydrolyze the more toxic S_P enantiomers, and selected mutants were tested with GB and GD to assess the utility of the analogues in predicting the properties against authentic nerve agents.

MATERIALS AND METHODS

Materials. *Escherichia coli* BL21(DE3) and XL1-blue cells were purchased from Stratagene. Expression plasmid pET20b(+) was obtained from Invitrogen. The bacterial phosphotriesterase and the site-directed mutants (G60A, I106G, F132G, S308G, I106G/H257Y, I106G/F132G/H257Y, I106A/F132A/H257Y, I106A/H257Y/S308A, and H254G/H257W/L303T) were purified to homogeneity as previously described (*13*, *14*, *18*). The H254Q/H257F mutant was isolated from a H254X/H257X library (*18*, *19*), and the H257Y/L303T mutant was identified within a H254X/H257X/L303T library (*17*). In each case, H254 and H257 were completely randomized to generate 400 possible permutations with 20 different amino acids at each of the two targeted sites. Nearly 1000 colonies from each library were isolated and screened for catalytic activity. The H254Q/H257F mutant was initially identified as being beneficial by screening with Demeton-S, an analogue of VX. The H257Y/L303T mutant was isolated by screening with the S_P enantiomers of compounds **2** and **4**.

Synthesis of Racemic Substrates. The corresponding alcohol (1 equiv) was dissolved in ethyl ether (~100 mL) and cooled in a dry ice/acetone bath. Butyllithium (1 equiv) was added to the solution while the mixture was stirred. A solution of methylphosphonic dichloride (1 equiv) in ethyl ether (100 mL) was cooled in a dry ice/acetone bath for 10 min and added to the alcohol solution, and then the mixture was stirred at room temperature for an additional 4 h. One equivalent of 4-acetylphenol and triethylamine (1.2 equiv) were added to the reaction mixture, and the mixture was stirred for 8 h. The solution was washed with water (2 × 50 mL and 1 × 10 mL) and subsequently dried with anhydrous magnesium sulfate. After removal of the solvent, the crude product was purified by silica gel chromatography to yield the 4-acetylphenyl methylphosphonates (compounds **1**−**5**) in yields of 38−87%. The structures of compounds **1**−**5** were verified by mass spectrometry and ^{1}H NMR and ^{31}P NMR spectroscopy. The ^{1}H and ^{31}P NMR spectra were recorded on a Varian Unity INOVA 300 spectrophotometer with residual $CDCl_3$ as the internal reference for ^{1}H NMR and H_3PO_4 (85% in water) as the external reference for ^{31}P NMR. Exact mass measurements were taken on a PE Sciex APJ Qstar Pulsar mass spectrometer by the Laboratory for Biological Mass Spectrometry at Texas A&M University.

Isolation of S_P Enantiomers. The S_P enantiomers of compounds **1**−**5** were obtained by kinetic resolution of the

corresponding racemic compounds using the G60A mutant of PTE. The reactions were conducted at room temperature in a methanol/water solution (20%) with 50 mM CHES buffer (pH 9.0). The concentration of the racemic phosphonate was approximately 1.0 g/L. The reactions were monitored by measuring the formation of 4-acetylphenol at 294 nm and were stopped when no further increase in the absorbance was observed. The S_P enantiomers were extracted from the reaction mixture with chloroform. The chloroform solutions were dried with sodium sulfate and condensed to dryness to yield the final product. The S_P enantiomer of **1** was obtained in a yield of 83%, and the S_P enantiomers of **2**−**5** were obtained in yields greater than 91%. The enantiomeric excess (ee) was determined using the relative intensities of the ^{31}P NMR signals in the presence of Fmoc-Trp(Boc)-OH (*19*). The ee value for the isolation of the S_P enantiomer of **1** was 95%, and for compounds **2**−**5**, the ee values were 99% (*20*).

Isolation of R_P Enantiomers. The R_P enantiomers of compounds **1**−**5** were obtained by kinetic resolution of the racemic compounds using various PTE mutants. The reactions were conducted at room temperature in a methanol/water solution (20%) containing 50 mM CHES buffer (pH 9.0). The concentrations of the racemic phosphonates were ~1.0 g/L. The R_P enantiomer of compound **1** was obtained using 4.2 mg of the PTE mutant H257Y/L303T, and the isolated yield was 52% with an ee value of 98%. The R_P enantiomer of compound **2** was obtained using 4.2 mg of the PTE mutant H257Y/L303T. The yield was 74%, and the ee value was 98%. The R_P enantiomer of compound **3** was obtained using 7.2 mg of the mutant I106A/H257Y/S308A. The yield was 48%, and the ee value was 99%. The R_PR_C and R_PS_C enantiomers of compound **4** were obtained using 6.3 mg of the mutant H257Y/L303T. The yields were 98 and 99%, respectively. The ee values were 99% for both the R_PR_C and R_PS_C enantiomers of compound **4**. The R_P enantiomer of compound **5** was obtained using 1.8 mg of the mutant I106G/F132G/H257Y. The yield was 48%, and the ee value was 97%. The ee values were determined on the basis of the relative intensities of the ^{31}P NMR signals in the presence of Fmoc-Trp(Boc)-OH (*20*).

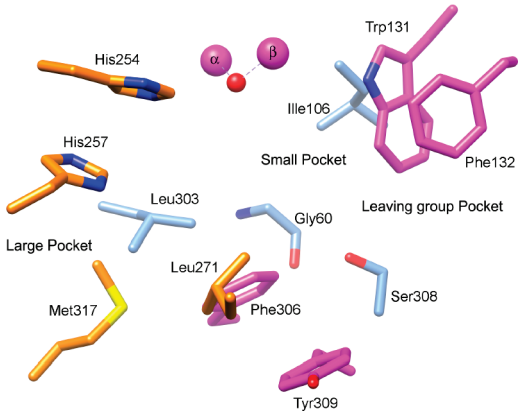

FIGURE 1: Graphic representation of the binding pockets within the active site of PTE. The small pocket consists of Gly-60, Ile-106, Leu-303, and Ser-308. The large pocket consists of His-254, His-257, Leu-271, and Met-317. The leaving group pocket is surrounded by Trp-131, Phe-132, Phe-306, and-Tyr 309.

Expression, Growth, and Preparation of Wild-Type and Mutant Enzymes. The gene for the expression of PTE was cloned between the *Nde*I and *Eco*RI sites of a pET20b(+) plasmid. The plasmids for the expression of the wild-type and mutant enzymes were transformed into BL-21(DE3) cells (*9*). The cells were inoculated in Luria-Bertani (LB) broth and grown overnight at 37 °C. The overnight cultures were incubated in Terrific Broth (TB) containing 100 μg/mL ampicillin and 1.0 mM $CoCl_2$ at 30 °C. The expression of PTE was induced by the addition of 1.0 mM IPTG when the OD_{600} reached 0.4. The cells were harvested at 4 °C by centrifugation after the culture was allowed to reach the stationary phase after 36−42 h at 30 °C. All subsequent steps were conducted at 4 °C. The isolated cells were suspended with 10 mM HEPES (pH 8.5) and lysed with a 5 s pulsed sonication for 24 min at 0 °C at the medium power setting using a Heat System-Ultrasonics, Inc. (Farmington, NY), model W830 ultrasonic processor. The lysed cell suspensions were combined and centrifuged at 13000*g* for 15 min. The supernatant fluid was decanted, and then a solution of protamine sulfate (2%, w/v) was added dropwise over a 20 min period while the mixture

Scheme 3: Structures of Organophosphate Substrates

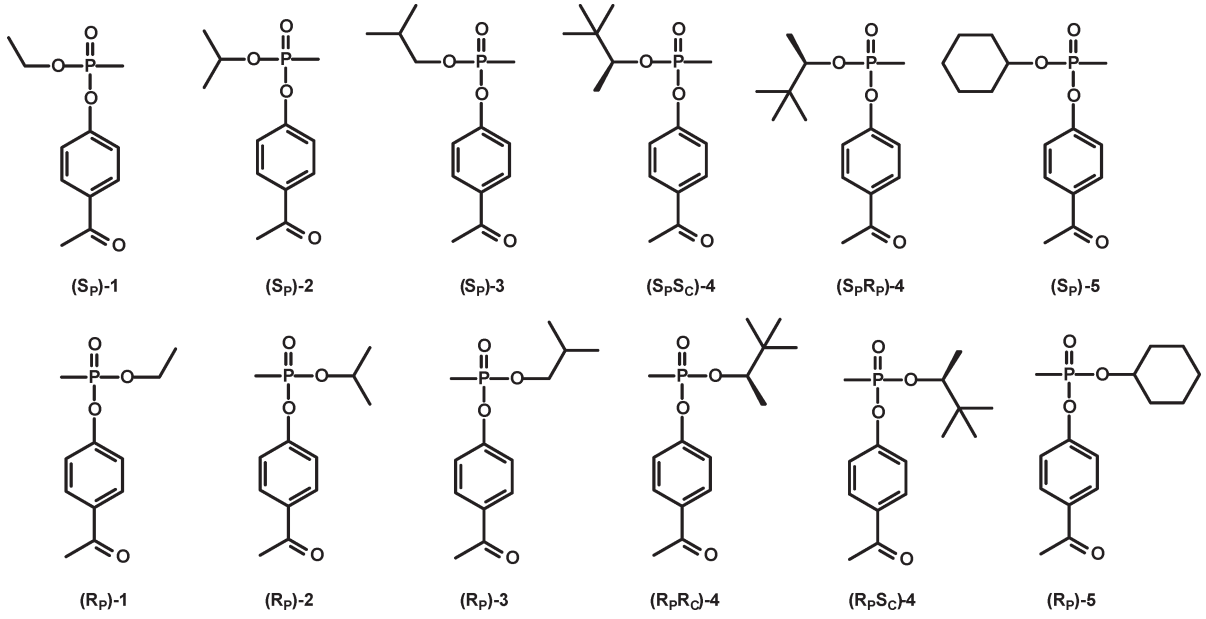

was stirred until the protamine sulfate concentration reached 0.4%. The supernatant solution was subjected to ammonium sulfate fractionation by the addition of solid ammonium sulfate to 60% saturation (371 mg/mL) while the mixture was stirred for 30 min and then kept stirring for an additional 45 min. The pellet was collected by centrifugation at 13000*g* for 30 min, and the protein was recovered by dissolving the precipitate in 3 mL of buffer. The protein was loaded onto a 5.0 cm × 150 cm gel filtration column containing Ultrogel AcA 54 (IBF, Columbia, MD) and eluted at a flow rate of 1.0 mL/min. The fractions were pooled on the basis of the enzymatic activity and absorbance at 280 nm and then applied to a 5 cm × 25 cm column, containing DEAE-Sephadex A-25 previously equilibrated with 10 mM HEPES (pH 8.5). SDS−polyacrylamide gel electrophoresis demonstrated that all of the mutant enzymes were the same size as the wild-type PTE and that the purity of all proteins was greater than 95%.

Spectrophotometric Enzyme Assays. The kinetic constants for each substrate were determined by monitoring the formation of *p*-acetylphenol at 294 nm ($\varepsilon = 7710\ M^{-1}\ cm^{-1}$) at 30 °C using a SpectraMax plate reader (Molecular Devices Inc., Sunnyvale, CA). The assay mixtures contained 50 mM CHES (pH 9.0), 100 μM $CoCl_2$, and various concentrations of substrates. The reactions were initiated by the addition of enzyme. Because of the limited solubility of compounds **4** and **5**, 10% methanol (v/v) was added to the assay mixtures.

Enzymatic Assays for GB and GD. Wild-type PTE and the variants G60A, S308G, H257Y/L303T, and H254G/H257W/L303T were purified to homogeneity and stored at −80 °C prior to use. The time courses for the enzymatic hydrolysis of GB and GD were obtained by following the heat of reaction using a MicroCal (Northampton, MA) iTC_{200} isothermal titration calorimeter (ITC), with a 200 μL reaction cell. All reactions were conducted by injection of the phosphonofluoridate into the enzyme solution at 25 °C with a reference offset of 5 μcal/s, a syringe stirring speed of 1000 rpm, a preinjection delay of 180 s, and a 5 s recording interval. The enzymes were diluted into 10 mM potassium phosphate (pH 7.4) for GB or 30 mM potassium phosphate (pH 7.4) for GD. The final concentration of GB for all experiments was 250 μM. The final concentration of GD for all experiments was 300 μM. The total heat of hydrolysis for GB (50 nmol) was determined by following the reaction catalyzed by 20 nM G60A and 80 nM H254G/H257W/L303T to completion. The total heat of hydrolysis of GD (60 nmol) was determined by following the reaction catalyzed by 200 nM wild-type PTE, 200 nM G60A, and 600 nM H254G/H257W/L303T to completion.

To isolate the deferential hydrolysis of individual enantiomers with PTE variants, the hydrolysis reactions were conducted with high and low concentrations of the enzyme. The hydrolysis of racemic GD with each variant was also analyzed by gas chromatography with a chiral separation column as previously described (*21*). Reaction solutions were removed from the ITC cell and mixed with an equal volume of dry ethyl acetate to extract the remaining agent. Aliquots (1 μL) of the organic phase were injected into the gas chromatograph for analysis.

Data Analysis. The kinetic constants (k_{cat} and k_{cat}/K_m) were obtained from a fit of the data to eq 1

$$v/E_t = k_{cat}[A]/(K_m + [A]) \quad (1)$$

where v is the initial velocity, k_{cat} is the turnover number, [A] is the substrate concentration, and K_m is the Michaelis constant. Estimates of k_{cat}/K_m for racemic GB and GD were obtained by transformation of the rate of heat applied for each ITC experiment. The ITC instrument records the instantaneous rate of heat applied to the reference cell to maintain thermal equilibrium at 5 s intervals. The rate of heat released during the enzymatic hydrolysis of these substrates was obtained by subtracting the experimental values from the baseline value at each time point. The total heat given off as a function of time was obtained by manual integration using a geometric approximation method according to eq 2

$$H_i = \sum_{t=o}^{t=i} dU_i \times 5s \quad (2)$$

where H_i is the total heat observed at time i and dU_i is the instantaneous rate of heat produced by the reaction at each time period. The heat of complete hydrolysis of GB (−730 μcal) or GD (−930 μcal) was determined according to eq 2 as the value of H_i as the reaction catalyzed by variants of PTE went to completion. The fractional hydrolysis catalyzed by individual variants as a function of time was determined by dividing the total heat observed at each time period by the total expected heat. Plots of the fraction GB or GD hydrolyzed over time appear as exponential time courses. Depending on the agent or variant used, one or two phases could be observed and fit to eq 3 or 4, respectively

$$F = a(1 - e^{-k_1 t}) \quad (3)$$

$$F = a(1 - e^{-k_1 t}) + b(1 - e^{-k_2 t}) \quad (4)$$

where F is the fraction hydrolyzed, a and b are the magnitudes of the exponential phases, t is time, and k_1 and k_2 are the exponential components for each phase. The magnitude of the exponential components was allowed to float. Assuming the concentration of substrate is less than K_m, the value of k_{cat}/K_m was estimated from the exponentials according to eq 5

$$k_x/E_t = k_{cat}/K_m \quad (5)$$

where k_x is the exponential component and E_t is the enzyme concentration.

RESULTS

Selection of Mutants. Specific residues in the substrate binding pocket of PTE were targeted for mutagenesis. The smallest residue in the small subsite of PTE, Gly-60, was mutated to alanine to reduce the size of the small pocket. The small pocket and adjacent areas were also systematically enlarged by mutation of Ile-106, Ser-308, and Phe-132 to glycine or alanine. Other mutations combined alterations of the small and large subsites simultaneously. The catalytic activities of the wild-type and mutant enzymes with the compounds presented in Scheme 3 were determined, and the kinetic parameters are listed in Tables 1 and 2. The stereoselectivities of these enzymes using the isolated chiral enantiomers are listed in Table 3.

Catalytic Activity and Stereoselectivity of Wild-Type PTE. The values of k_{cat} and k_{cat}/K_m for wild-type PTE with compounds **2**−**5** demonstrate that this enzyme preferentially hydrolyzes the R_P enantiomers of these organophosphonates. There is, however, a slight preference for the S_P enantiomer of compound **1**. As the size of the substituent attached to the phosphorus center becomes larger, the preference for the R_P

Table 1: Turnover Numbers (k_{cat}, s^{-1}) for the Wild-Type and Mutant Forms of PTE

compd	WT	G60A	I106G	F132G	S308G	H254Q/ H257F	H257Y/ L303T	I106G/ H257Y	I106G/F132G/ H257Y	I106A/F132A/ H257Y	I106A/H257Y/ S308A	H254G/H257W/ L303T
R_P/S_P-**1**	3.9×10^2	1.6×10^2	1.8×10^2	1.8×10^2	–	3.8×10	1.7×10^2	4.8×10^2	1.5×10^2	7.9×10^2	2.3×10^3	2.7×10^2
R_P-**1**	1.5×10^2	1.3×10^2	6.8×10	6.8×10	1.1×10^2	1.7×10^2	7.3×10^0	8.9×10	3.4×10	–	2.0×10^2	1.4×10
S_P-**1**	6.7×10^2	1.1×10^2	3.0×10^2	3.0×10^2	2.9×10^2	3.2×10	4.1×10^2	6.8×10^2	3.5×10^2	9.0×10^2	1.4×10^3	1.9×10^2
R_P/S_P-**2**	9.7×10	1.1×10^2	3.9×10	2.9×10	1.8×10^2	1.2×10	3.2×10^2	5.9×10	5.3×10	1.6×10^2	6.5×10^2	1.2×10^2
R_P-**2**	1.0×10^2	1.2×10^2	4.0×10	3.9×10	2.5×10^2	4.8×10	1.8×10	4.7×10	–	4.5×10	1.3×10^2	–
S_P-**2**	4.0×10	7.4×10^0	2.8×10	1.6×10	1.5×10	7.2×10^0	3.7×10^2	1.0×10^2	4.8×10	5.1×10^2	3.4×10^2	9.2×10
R_P/S_P-**3**	5.4×10	4.7×10	4.9×10	3.5×10	1.2×10^2	1.1×10	1.3×10^2	4.7×10^2	–	6.3×10^2	6.7×10^2	4.7×10
R_P-**3**	9.3×10	3.7×10	3.1×10	2.8×10	1.1×10^2	7.0×10	5.1×10	8.4×10^0	–	–	2.2×10	2.0×10
S_P-**3**	2.2×10	–	4.8×10	2.5×10	1.2×10	6.3×10^0	1.0×10^2	2.1×10^2	2.3×10^2	2.3×10^2	5.3×10^2	5.0×10
$R_PR_C/R_PS_C/S_PR_C/S_PS_C$-**4**	2.1×10^0	4.1×10^0	1.2×10^0	–	1.1×10^0	1.3×10^0	2.4×10^0	2.4×10^{-1}	2.9×10^{-2}	4.3×10^{-1}	1.1×10^0	1.8×10
R_PR_C/S_PR_C-**4**	2.5×10^0	3.9×10^0	–	–	2.5×10^0	8.2×10^{-1}	3.0×10^0	4.8×10^{-1}	4.2×10^{-2}	5.0×10^{-1}	7.8×10^{-1}	1.1×10
R_PS_C/S_PS_C-**4**	6.1×10^{-1}	1.3×10^0	9.0×10^{-2}	1.3×10^{-1}	4.2×10^{-1}	4.2×10^{-1}	8.0×10^{-1}	1.6×10^{-2}	4.1×10^{-2}	1.1×10^{-1}	1.4×10^{-1}	4.6×10^0
R_PR_C-**4**	3.4×10^0	8.5×10^0	3.3×10^0	1.2×10	2.2×10^0	5.5×10^{-1}	4.1×10^{-1}	7.6×10^{-2}	4.9×10^{-2}	5.0×10^{-2}	1.7×10^{-1}	2.0×10^0
R_PS_C-**4**	4.5×10^{-1}	1.5×10^0	1.5×10^{-1}	1.5×10^{-1}	6.2×10^{-1}	1.7×10^{-1}	–	6.5×10^{-2}	5.5×10^{-3}	–	4.2×10^{-2}	2.1×10^{-1}
S_PR_C-**4**	7.7×10^{-1}	9.5×10^2	5.0×10^{-2}	3.2×10^{-1}	5.0×10^{-1}	6.3×10^{-1}	6.3×10^0	3.7×10^{-2}	1.6×10^{-1}	7.4×10^{-1}	1.0×10^0	1.2×10
S_PS_C-**4**	1.6×10^{-2}	–	–	1.2×10^{-1}	1.2×10^{-1}	3.3×10^{-1}	2.1×10^0	2.2×10^{-2}	5.3×10^{-2}	2.4×10^{-1}	3.5×10^{-1}	2.9×10^0
R_P/S_P-**5**	2.8×10	1.9×10	1.1×10	5.4×10^0	8.4×10	3.8×10	4.5×10^0	7.8×10^0	1.6×10	2.4×10^0	–	1.3×10
R_P-**5**	–	9.3×10	–	1.4×10	1.5×10^2	3.8×10	5.9×10^0	–	–	–	4.2×10^0	8.1×10^{-1}
S_P-**5**	–	–	5.1×10^0	3.3×10^{-1}	1.4×10^{-1}	–	5.1×10^0	1.8×10	1.3×10	4.7×10^0	4.5×10^0	1.9×10

Table 2: Values of k_{cat}/K_m (M^{-1} s^{-1}) for the Wild-Type and Mutant Forms of PTE

compd	WT	G60A	I106G	F132G	S308G	H254Q/ H257F	H257Y/ L303T	I106G/ H257Y	I106G/F132G/ H257Y	I106A/F132A/ H257Y	I106A/H257Y/ S308A	H254G/H257W/ L303T
R_P/S_P-**1**	7.2×10^5	2.7×10^5	9.4×10^4	2.2×10^5	9.8×10^4	1.9×10^6	7.6×10^4	1.8×10^5	8.3×10^4	1.6×10^5	2.6×10^5	7.8×10^4
R_P-**1**	4.9×10^5	5.2×10^5	6.2×10^4	3.5×10^4	7.5×10^4	1.5×10^6	2.4×10^3	3.3×10^4	6.3×10^3	6.9×10^3	6.0×10^4	1.5×10^3
S_P-**1**	1.2×10^6	1.3×10^5	7.7×10^4	3.3×10^5	1.5×10^5	7.1×10^6	1.6×10^5	3.8×10^5	1.1×10^5	3.5×10^5	7.2×10^5	2.2×10^5
R_P/S_P-**2**	2.4×10^5	2.5×10^5	3.3×10^4	2.7×10^4	5.4×10^4	8.4×10^5	3.9×10^4	1.2×10^4	4.9×10^3	3.0×10^4	3.1×10^4	4.0×10^4
R_P-**2**	5.8×10^5	5.2×10^5	5.8×10^4	5.9×10^4	1.1×10^5	8.2×10^5	2.5×10^3	8.9×10^3	1.5×10^3	2.3×10^3	1.9×10^4	1.8×10^3
S_P-**2**	2.7×10^4	6.2×10^3	3.3×10^3	5.5×10^3	3.1×10^3	1.2×10^6	1.1×10^5	3.0×10^4	6.8×10^3	5.0×10^4	6.7×10^4	5.9×10^4
R_P/S_P-**3**	2.7×10^5	5.2×10^5	5.4×10^4	8.3×10^4	1.1×10^5	5.2×10^5	5.3×10^4	6.0×10^4	3.6×10^4	5.9×10^4	1.7×10^5	9.9×10^4
R_P-**3**	8.5×10^5	7.6×10^5	6.2×10^4	1.2×10^5	1.8×10^5	3.1×10^5	1.3×10^4	2.3×10^3	4.5×10^2	4.9×10^2	9.5×10^3	1.5×10^3
S_P-**3**	3.4×10^4	9.9×10	4.4×10^4	3.6×10^4	9.5×10^3	1.6×10^6	7.3×10^4	1.5×10^5	9.1×10^4	1.3×10^5	3.9×10^5	1.8×10^5
$R_PR_C/R_PS_C/S_PR_C/S_PS_C$-**4**	3.8×10^2	8.2×10^2	7.1×10	1.6×10^2	5.0×10^2	2.8×10^2	7.3×10^2	2.6×10	7.6×10^0	6.2×10	1.2×10^2	1.9×10^3
R_PR_C/S_PR_C-**4**	5.4×10^2	1.6×10^3	1.5×10^2	1.7×10^2	7.4×10^2	5.5×10^2	9.3×10^2	3.1×10	8.8×10^0	1.3×10^2	1.7×10^2	3.3×10^3
R_PS_C/S_PS_C-**4**	1.2×10^2	2.6×10^2	2.8×10	2.3×10	2.1×10^2	6.3×10	3.1×10^2	3.9×10^0	2.8×10^0	1.7×10	2.3×10	7.7×10^2
R_PR_C-**4**	1.3×10^3	3.0×10^3	3.8×10^2	3.3×10^2	2.3×10^3	1.9×10^2	5.8×10	1.7×10	8.4×10^0	2.3×10	5.9×10	2.2×10^2
R_PS_C-**4**	2.0×10^2	5.9×10^2	5.0×10	4.5×10	4.9×10^2	5.5×10	1.6×10	2.3×10^0	1.1×10^0	1.2×10^0	4.5×10^0	1.3×10^2
S_PR_C-**4**	1.1×10^2	1.7×10	1.4×10	8.4×10	1.1×10^2	1.6×10^3	1.8×10^3	8.0×10^0	1.3×10	1.5×10^2	2.4×10^2	8.1×10^3
S_PS_C-**4**	3.2×10^0	1.1×10^0	1.0×10	5.2×10^0	6.7×10^0	6.2×10	2.5×10^2	2.1×10^0	4.5×10^0	2.2×10	3.0×10	1.7×10^3
R_P/S_P-**5**	7.4×10^3	9.6×10^3	3.6×10^3	1.9×10^3	1.4×10^4	3.2×10^3	2.9×10^3	1.1×10^3	1.5×10^3	4.4×10^2	4.0×10^2	1.5×10^4
R_P-**5**	1.6×10^4	2.1×10^4	4.9×10^3	2.9×10^3	2.8×10^4	5.2×10^3	1.9×10^3	3.8×10^2	5.2×10	7.5×10	8.4×10^2	2.5×10^2
S_P-**5**	2.1×10	9.4×10^{-1}	8.4×10^2	8.1×10	1.0×10^2	3.3×10^2	5.8×10^3	2.6×10^3	4.6×10^3	1.0×10^3	5.7×10^2	2.8×10^4

Table 3: Ratios of k_{cat}/K_m for the Hydrolysis of Chiral Substrates by the Wild-Type and Mutant Forms of PTE

	R_P:S_P for **1**	R_P:S_P for **2**	R_P:S_P for **3**	R_PR_C:R_PS_C:S_PR_C:S_PS_C for **4**	R_P:S_P for **5**
wild-type	1:2	22:1	25:1	400:63:35:1	760:1
G60A	4:1	84:1	7600:1	3600:700:20:1	23000:1
I106G	1:1	18:1	1:1	38:5:1.5:1	6:1
F132G	1:9	11:1	3:1	64:8:16:1	35:1
S308G	1:2	34:1	19:1	340:73:17:1	280:1
H254Q/H257F	1:5	1:2	1:5	3:1:29:1	16:1
H257Y/L303T	1:64	1:44	1:6	4:1:120:16	1:3
I106G/H257Y	1:12	1:3	1:64	8:1:3:1	1:7
I106G/F132G/H257Y	1:18	1:5	1:200	7:1:11:4	1:89
I106A/F132A/H257Y	1:51	1:22	1:270	19:1:120:19	1:14
I106A/H257Y/S308A	1:12	1:4	1:41	13:1:54:7	2:1
H254G/H257W/L303T	1:140	1:33	1:120	2:1:65:14	1:110

enantiomer becomes stronger. For example, with compound **2**, the ratio for $^{R/S}(k_{cat}/K_m)$ is 22, whereas for compound **5**, the enantiomeric preference increases to 760.

Enhancement of Stereoselectivity. Gly-60 was originally mutated to an alanine residue in an attempt to decrease the size of the cavity for the binding of substrates in the active site of PTE. The values of k_{cat} and k_{cat}/K_m for the slow S_P enantiomers with G60A are decreased up to 340-fold relative to those of the wild-type enzyme. In addition, the kinetic constants for the R_P enantiomers of **4** and **5** are increased relative to those of the wild-type enzyme. The highest values of k_{cat}/K_m were obtained for the two R_P enantiomers of **4**. The G60A mutant has an enhanced stereoselectivity relative to that of the wild-type enzyme. The most extreme case is for compound **5**, where the R_P enantiomer is preferred by a factor of 2×10^4.

Relaxation of Stereoselectivity. The mutation of single residues in the small or leaving group pockets of PTE to amino acids with smaller side chains results in an active site that is somewhat larger than that of the wild-type enzyme. In general, this perturbation to the active site results in the relaxation of stereoselectivity through an enhancement of the rate of the initially slower S_P enantiomers. For example, the I106G mutant diminishes the stereoselectivity for compounds **1** and **3**−**5** relative to wild-type PTE. The F132G mutant relaxes the stereoselectivity for compounds **2**−**5** compared with wild-type PTE. Thus, single mutations in the small or leaving group pockets to glycine residues relax the stereoselectivity of the mutants relative to wild-type PTE.

Reversal of the Stereoselectivity. The mutants with a relaxed enantioselectivity contain an expanded small pocket. Modification of the large and small pockets simultaneously inverts the inherent stereoselectivity relative to that of wild-type PTE. The mutants H257Y/L303T, I106G/H257Y, I106G/F132G/H257Y, I106A/F132A/H257Y, and I106A/H257Y/S308A all have residues in the small pocket (Ile-106, Phe-132, and Ser-308) that are replaced with either glycine or alanine. In addition, these mutants include changes to His-257 in the large pocket. For example, wild-type PTE prefers the R_P enantiomer of compound **3** by a factor of 25, whereas the I106A/F132A/H257Y mutant inverts the stereoselectivity with compound **3** and prefers the S_P enantiomer by a factor of 260.

The H254G/H257W/L303T mutant contains an extended small pocket and a modified large pocket. This mutant has a more distinct effect on the reversal of stereoselectivity than the other mutants for the hydrolysis of compounds **1** and **5**. For these compounds, the S_P enantiomers are preferred by factors of 140 and 110, respectively. In addition to an inversion of enantioselectivity relative to that of the wild-type enzyme, the H254G/H257W/L303T mutant exhibits the highest overall catalytic activity for the more toxic S_P enantiomers of compounds **4** and **5**. The values of k_{cat}/K_m for the hydrolysis of the S_PR_C and S_PS_C stereoisomers of compound **4** are enhanced 74- and 540-fold, respectively, relative to that of the wild-type enzyme. The most notable case is that for the S_P enantiomer of compound **5** with a k_{cat}/K_m that is more than 3 orders of magnitude higher than that of the wild-type enzyme. The reversal in stereoselectivity, relative to that of the G60A mutant, for the hydrolysis of racemic **5** is shown in Figure 2. The addition of H254G/H257W/L303T hydrolyzes approximately 50% of the total material in ~5 min, and then the addition of G60A hydrolyzes the remaining material.

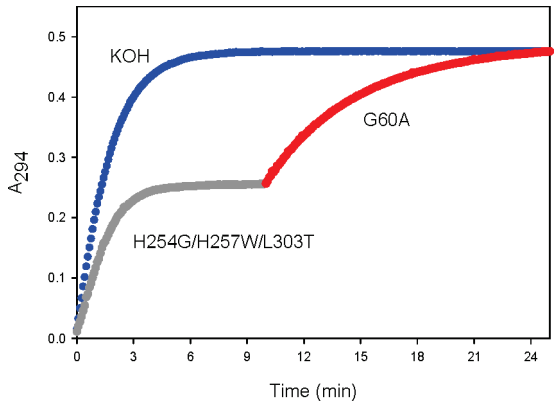

FIGURE 2: Time course for the hydrolysis of racemic **5** using two mutants of PTE. The total concentration of compound **5** was determined by the complete hydrolysis using 0.1 M KOH. The hydrolysis of the S_P enantiomer of racemic **5** was initiated with 165 nM H254G/H257W/L303T PTE. After 10 min, the G60A mutant of PTE was added to hydrolyze the R_P enantiomer.

Hydrolysis of Racemic GB and GD. Wild-type PTE is known to prefer the less toxic R_P enantiomers of nerve agents GB and GD (*16*). PTE mutants with differing catalytic properties with the analogues to these compounds (**2** and **4**, respectively) were selected for testing with racemic GB and GD. Because of regulatory considerations on the maximum allowable concentrations of these two nerve agents, the enzymatic reactions were followed via ITC for the complete hydrolysis at a single fixed concentration of agent. The PTE mutants were tested under identical reaction conditions for their ability to hydrolyze 250 μM GB and 300 μM GD in 200 μL reaction volumes. The values of k_{cat}/K_m for each mutant were determined from the exponential phases for hydrolysis of the racemic mixtures and are reported in

Table 4: Values of k_{cat}/K_m (M^{-1} s^{-1}) for Wild-Type and Mutant Forms of PTE against Nerve Agents GB and GD

	GB		GD		
compd	k_{cat}/K_m1[a]	k_{cat}/K_m2	k_{cat}/K_m1	k_{cat}/K_m2	enantiomeric preference[b]
wild-type	$(9 \pm 3) \times 10^4$		$(2.6 \pm 0.2) \times 10^3$		$R_PS_C, R_PR_C, S_PR_C \gg S_PS_C$
G60A	$(1.2 \pm 0.1) \times 10^5$	$(2.66 \pm 0.01) \times 10^4$	$(2.5 \pm 0.3) \times 10^4$	$(2.2 \pm 0.3) \times 10^3$	$R_PS_C, R_PR_C > S_PS_C, S_PR_C$
S308G	$(3.9 \pm 0.9) \times 10^4$		$(9.1 \pm 0.5) \times 10^3$	$(8 \pm 2) \times 10^2$	$R_PR_C, R_PS_C > S_PR_C \gg S_PS_C$
H254G/H257W/L303T	$(1.5 \pm 0.1) \times 10^4$	$(9.7 \pm 0.1) \times 10^2$	$(2.2 \pm 0.2) \times 10^3$		$S_PS_C, S_PR_C \gg R_PS_C, R_PR_C$
H275Y/L303T	$(3 \pm 1) \times 10^5$	$(3.65 \pm 0.01) \times 10^4$	$(8.9 \pm 0.9) \times 10^4$	$(6.8 \pm 0.2) \times 10^3$	$S_PS_C, S_PR_C > R_PS_C, R_PR_C$

[a] k_{cat}/K_m1 and k_{cat}/K_m2 were determined from the first and second exponential phases, respectively, during the reaction of GB or GD as followed by ITC. [b] First phase > second phase ≫ not observed.

Table 4. Representative time courses for the hydrolysis of GB are given in Figure 3.

The fractional hydrolysis of GB catalyzed by wild-type PTE fits to a single exponential (Figure 3a and Table 4). Similarly, the ITC traces for the S308G mutant with GB (data not shown) can be fit to a single exponential (Table 4). The time courses for three other mutants (G60A, H254G/H257W/L303T, and H257Y/L303T) could not be fit to a single exponential, indicating that the two enantiomers were hydrolyzed at different rates. G60A has a value of k_{cat}/K_m for the first phase that is similar to that observed with the wild-type enzyme and a second phase that is ~5-fold slower (Figure 3b and Table 4). The value of k_{cat}/K_m for the H254G/H257W/L303T mutant, obtained from the first phase, is reduced in value relative to that of the wild-type enzyme, and a second phase that is reduced by ~2 orders of magnitude (data not shown). H257Y/L303T has the highest value of k_{cat}/K_m observed for the hydrolysis of GB (3×10^5 M^{-1} s^{-1}) and a clear second phase that was approximately 10-fold slower (Figure 3c).

The racemic GD used in these experiments contained four diastereomers that can be separated by chiral gas chromatography (Figure 4). In all of the enzymatic time courses, only one or two phases could be clearly distinguished from one another. Representative plots are given in Figure 5. To determine which enantiomers were being degraded in each phase, the substrates remaining after selected ITC experiments were extracted with ethyl acetate and separated by gas chromatography to identify the remaining isomers. At high enzyme concentrations, wild-type PTE exhibited a single-exponential phase with an estimated value of k_{cat}/K_m that is reduced from that obtained with GB (Figure 5a and Table 4). The gas chromatographic separation indicated that the two R_P enantiomers were almost completely hydrolyzed along with the S_PR_C enantiomer, leaving only the S_PS_C enantiomer in the reaction mixture (Figure 5b). The G60A variant exhibited two phases in the ITC experiment, with the faster phase having a k_{cat}/K_m value nearly 1 order of magnitude higher than that obtained with wild-type PTE (Figure 5c). Gas chromatographic analysis revealed that the faster phase corresponded primarily to the degradation of the two R_P enantiomers, while the two S_P enantiomers only begin to be degraded in the second phase (Figure 5d). The S_PS_C diastereomer is hydrolyzed more slowly than the S_PR_C stereoisomer by G60A. The H254G/H257W/L303T mutant exhibited a single-exponential phase with a value of k_{cat}/K_m similar to that observed with wild-type PTE (Figure 5e). However, the gas chromatographic separation indicates that the diastereomeric preference is inverted because the S_PS_C and S_PR_C diastereomers are hydrolyzed significantly faster than the R_PR_C and R_PS_C stereoisomers (Figure 5f). The H257Y/L303T mutant has the highest value of k_{cat}/K_m for the hydrolysis of GD with the hydrolysis of the two S_P enantiomers in the first phase and the two R_P enantiomers in the second phase

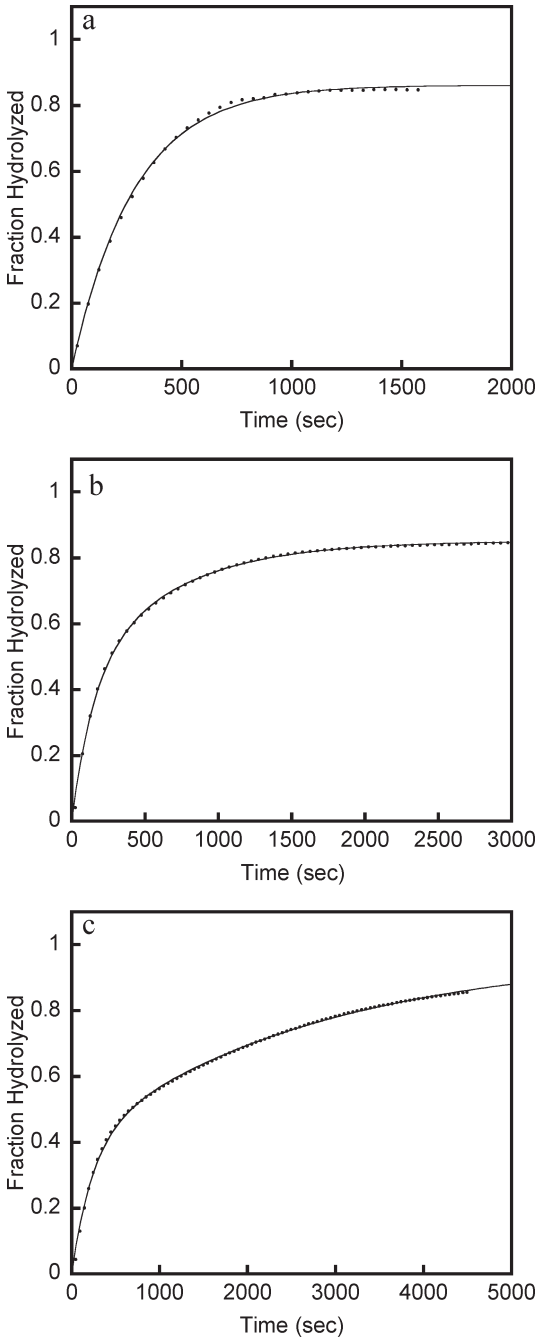

FIGURE 3: Hydrolysis of 250 μM racemic GB followed by ITC. All reactions were initiated by injection of 5 μL of GB into a volume of 200 μL and followed with a MicroCal iTC$_{200}$ isothermal calorimeter. (A) Hydrolysis of racemic GB by 30 nM wild-type PTE as a function of time. The data are fit to single exponential. (B) Hydrolysis of GB by 60 nM G60A as a function of time. The data are fit to the sum of two exponentials. (C) Hydrolysis of racemic GB by 10 nM H257Y/L303T as a function of time. The data are fit to the sum of two exponentials.

(Figure 5g). The S308G mutant also exhibited two phases in time course experiments (data not shown), with the first phase having a k_{cat}/K_m value enhanced relative to that of the wild-type enzyme and a second phase reduced by ~1 order of magnitude.

DISCUSSION

Phosphotriesterase possesses broad substrate specificity and a tunable stereoselectivity that can be harnessed for the detoxification of chemical warfare agents such as GA, GB, GD, GF, VX, and VR. These nerve agents contain a chiral phosphoryl center, and the toxicity of the individual stereoisomers differs substantially. Wild-type PTE preferentially hydrolyzes the less toxic R_P stereoisomers of these organophosphorus nerve agents and the analogues prepared for this investigation (*16*, *22*). Compounds **1**−**5** were developed as readily prepared analogues of the G and V agents that can be isolated with chiral purities of 95−99% ee. These compounds can also be used in high-throughput screening trials for the rapid identification of enzyme mutants that are enhanced in the catalytic hydrolysis of the most toxic stereoisomers.

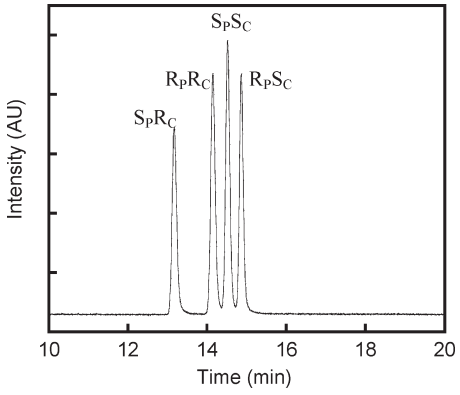

FIGURE 4: Separation of stereoisomers of racemic GD by gas chromatography.

The inherent stereoselectivity of wild-type PTE for the R_P enantiomers of compounds **1**−**5** increases with the size of the large substituent attached directly to the phosphorus center. Site specific mutations to the active site of wild-type PTE have demonstrated that the kinetic constants for the hydrolysis of individual compounds can be significantly enhanced by the direct manipulation of the relative size of the large and small subpockets within the active site of this enzyme. For example, substitution of an alanine for a glycine residue in the small pocket significantly enhances the stereochemical preference, $^{R/S}(k_{cat}/K_m)$, for all of the compounds tested. With this mutant, the stereochemical selectivity is enhanced while maintaining a relatively high turnover for the preferred R_P enantiomer.

A significant number of the variants tested for this investigation exhibited an enhanced ability to degrade the S_P stereoisomers of the nerve agent analogues. The dramatic improvements in the catalytic constant, k_{cat}/K_m, for the S_P enantiomers of compounds **2**−**5** are graphically illustrated in Figure 6. The best variant of PTE with the S_P enantiomers of compounds **2** and **3**, H254Q/H257F, is enhanced by nearly 2 orders of magnitude relative to the wild-type enzyme. For compounds **4** and **5**, the best mutant tested is H254G/H257W/L303T. With the S_PR_C enantiomer of analogue **4**, this mutant is enhanced by a factor of 74, and for the S_PS_C isomer, the enhancement, relative to the wild-type enzyme, is 540. For compound **5**, the enhancement is even greater; the H254G/H257W/L303T mutant hydrolyzes the S_P enantiomer of analogue **5** more than 3 orders of magnitude faster than the wild-type enzyme. For compounds **3**−**5** the second best mutant identified to date is the H257Y/L303T mutant.

The utilization of nerve agent analogues simplifies the identification of enzyme variants with the desired ability to hydrolyze the most toxic enantiomers of GB, GD, and GF. However, it is

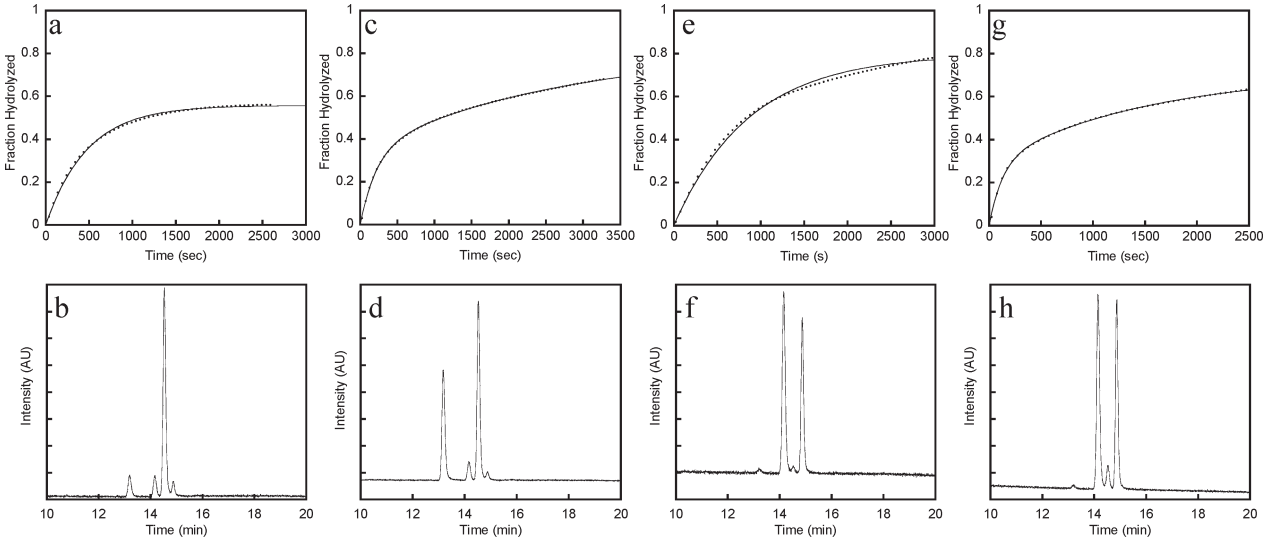

FIGURE 5: Hydrolysis of 300 μM GD. All reactions were conducted in a volume of 200 μL and initiated by the injection of 6 μL of GD into the enzyme solution. Hydrolysis of GD (panels A, C, E, and G) was followed by monitoring the heat liberated as a function of time. Following each experiment, the unreacted fraction of GD was analyzed by gas chromatography with a chiral separation column (panels B, D, F, and H). The order of elution from the gas chromatography column was as follows: S_PR_C (13 min), R_PR_C (14.1 min), S_PS_C (14.5 min), R_PS_C (15 min). (A) Hydrolysis of GD by 800 nM wild-type PTE as a function of time. The line is fit to a single exponential. (B) Analysis of the GD remaining following reaction with wild-type PTE. (C) Hydrolysis of GD by 200 nM G60A as a function of time. The line is a fit to the sum of two exponentials. (D) Analysis of unreacted GD following reaction with G60A. (E) Hydrolysis of GD by 600 nM H254G/H257W/L303T as a function of time. The line represents a fit of the data to a single exponential. (F) Analysis of the uneacted GD remaining following reaction with H254G/H257W/L303T. (G) Hydrolysis of GD by 100 nM H257Y/L303T as a function of time. The line is a fit to the sum of two exponentials. (H) Analysis of the unreacted GD remaining following reaction with H257Y/L303T.

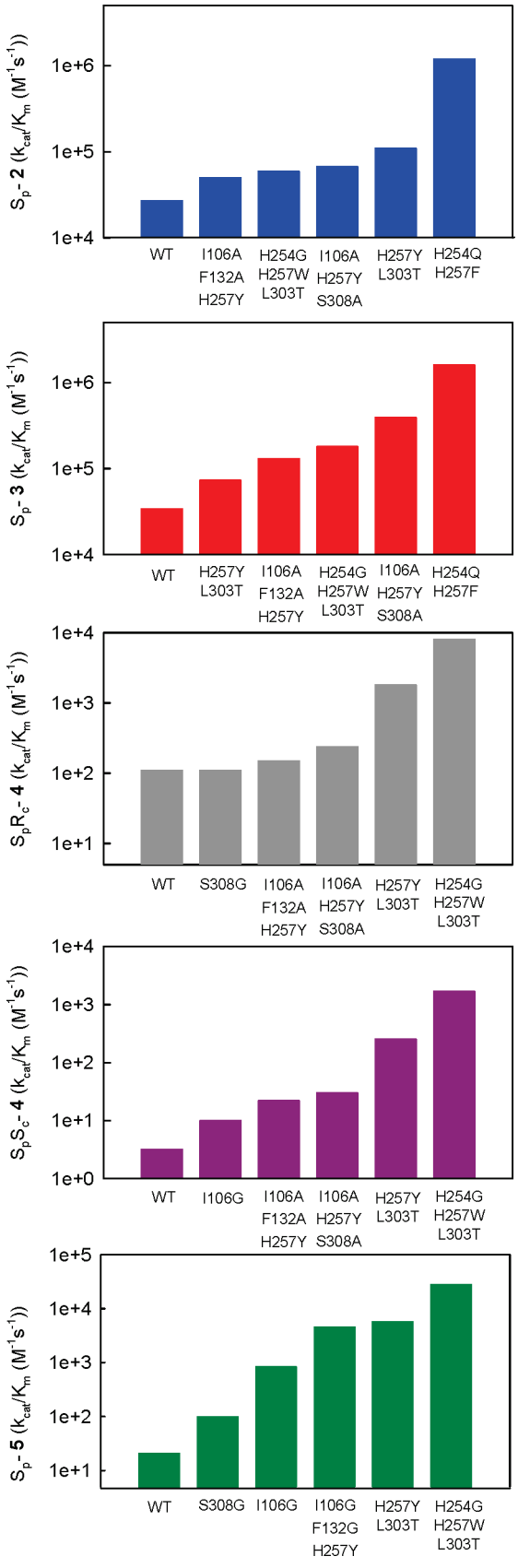

FIGURE 6: Bar graph illustrating changes in the value of k_{cat}/K_m for the S_P enantiomers of compounds **2**−**5** catalyzed by the wild-type and mutant forms of PTE.

important that the nerve agent stereoselectivity of mutant enzymes be determined by assessing hydrolysis of authentic nerve agent enantiomers. The k_{cat}/K_m values for nerve agents GB and GD were determined for a select group of site-specific mutations to the active site of PTE. The values of k_{cat}/K_m reported in Table 4 were obtained from the time courses for the hydrolysis of the racemic mixtures at a single fixed concentration of GB or GD. It must be noted, however, that the values reported in some cases are derived from the composite hydrolysis of multiple enantiomers and thus represent a weighted average of the kinetic constants. It is also assumed in these studies that the initial substrate concentrations for these assays are less than the K_m. However, all of the mutants were tested under identical conditions, allowing for a direct comparison of the observed kinetic properties, and thus, this assumption will have relatively little influence on the overall conclusions.

Under the experimental conditions employed for this investigation, only a single first-order rate constant for the hydrolysis of racemic GB could be obtained with wild-type PTE. The mutant G60A, which shows more stereochemical selectivity against the analogue of GB (compound **2**), clearly shows differential rates of hydrolysis using racemic GB. The value of k_{cat}/K_m for the faster enantiomer (presumably the R_P enantiomer) is approximately 4-fold lower than the value of k_{cat}/K_m for the R_P enantiomer of compound **2**. The mutant S308G did not display a measurable rate differential for hydrolysis of the two enantiomers of GB. The single mutation in this variant is located in the leaving group pocket, and it is likely that the significant difference in the leaving group between analogue **2** and GB is a contributing cause for the differing characteristics. The remaining variants (H257Y/L303T and H254G/H257W/L303T) exhibit greater stereochemical selectivity with compound **2** than the wild-type enzyme. These two mutants also exhibited differential rates of hydrolysis of the two stereoisomers of GB that mirror the differences in the values of k_{cat}/K_m with analogue **2**. The best enzyme identified for the hydrolysis of GB is H257Y/L303T. The value of k_{cat}/K_m for the fastest enantiomer of GB (3×10^5 M^{-1} s^{-1}) matches quite well with the value of k_{cat}/K_m for the S_P enantiomer of analogue **2** (1.1×10^5 M^{-1} s^{-1}).

The experiments with GD are complicated by the presence of four stereoisomers. Under the conditions used, no more than two distinct phases could be observed in the time courses for the enzymatic hydrolysis of GD. Gas chromatography was utilized concurrently with the ITC measurements to determine the specific stereoisomers that were preferentially hydrolyzed in the early phases of these reactions. The time course for the hydrolysis of GD by wild-type PTE could be fit to a rate equation with a single exponential that appears to be due to the hydrolysis of three of the four stereoisomers. The stereoselective preferences measured with analogue **4** show an only 10-fold difference in the values of k_{cat}/K_m among the three fastest stereoisomers. The slowest stereoisomer of compound **4** (S_PS_C) is hydrolyzed by wild-type PTE ~35-fold slower than the next fastest stereoisomer (S_PR_C). The diastereomeric preference determined by gas chromatography indicated that the two R_P stereoisomers, along with the S_PR_C enantiomer of GD, were the preferred substrates.

Differential rates of hydrolysis were detected in the hydrolysis of racemic GD by mutant G60A. Hydrolysis of the two R_P enantiomers was preferred. The measured values of k_{cat}/K_m for the two R_P enantiomers with G60A were significantly improved over that of the wild-type enzyme as was also observed with analogue **4**. The hydrolysis reaction catalyzed by S308G exhibited two phases in the time courses, with the first phase due to the two R_P stereoisomers and the second phase dominated by the hydrolysis of the S_PR_C enantiomer. The kinetic measurements

with the nerve agent analogues indicated that k_{cat}/K_m should be enhanced over that of wild-type PTE, which was observed. The H254G/H257W/L303T mutant exhibited a single phase during the hydrolysis of racemic GD. This phase is dominated by the hydrolysis of the two S_P stereoisomers. The observed value of k_{cat}/K_m was in rough agreement with that obtained for the hydrolysis of the racemic GD by the wild-type enzyme, but this mutant is significantly enhanced in the hydrolysis of the two most toxic stereoisomers.

The reaction catalyzed by the H257Y/L303T mutant exhibited two exponential phases during the time courses for the hydrolysis of racemic GD, with the faster phase being the hydrolysis of the two S_P diastereomers and the slower phase being due to the hydrolysis of the two R_P diastereomers. The values of k_{cat}/K_m for the hydrolysis of racemic GD were significantly higher than what was predicted from the investigations with the nerve agent analogues.

The use of the nerve agent analogues greatly simplifies the identification of PTE variants with improved ability to hydrolyze the more toxic stereoisomers of the authentic nerve agents GB and GD. While the results with analogues and the specific nerve agents are not identical, these results indicate that the findings with analogues accurately predict improvements against GB and GD. Comparison of the results obtained with the nerve agents GB and GD and their respective analogues indicates that these compounds may provide a more stringent test of the stereochemical preferences of PTE based on the phosphoryl center. The changes in k_{cat}/K_m obtained with the analogues are largely reflected in the values of k_{cat}/K_m found with the authentic nerve agents. These strategies have allowed the isolation of variants that are significantly improved for the hydrolysis of both GB and GD and with a stereochemical preference for the more toxic S_P stereoisomers.

REFERENCES

1. Ecobichon, D. J. (2001) Casarett and Doull's Toxicology: The basic science of poisons, 6th ed., pp 763−810, McGraw-Hill, New York.
2. Benschop, H. P., and Dejong, L. P. A. (1988) Nerve agent stereoisomers: Analysis, isolation, and toxicology. *Acc. Chem. Res. 21*, 368–374.
3. Worek, F., Szinicz, L., Eyer, P., and Thiermann, H. (2005) Evaluation of oxime efficacy in nerve agent poisoning: Development of a kinetic-based dynamic model. *Toxicol. Appl. Pharmacol. 209*, 193–202.
4. Josse, D., Xie, W., Renault, F., Rochu, F., Schopfer, L. M., Masson, P., and Lockridge, O. (1999) Identification of Residues Essential for Human Paraoxonase (PON1) Arylesterase/Organophosphatase Activities. *Biochemistry 38*, 2816–2825.
5. Hartleib, J., and Ruterjans, H. (2001) High-yield expression, purification, and characterization of the recombinant diisopropylfluorophosphatase from *Loligo vulgaris*. *Protein Expression Purif. 21*, 210–219.
6. Wang, F., Xiao, M. Z., and Mu, S. F. (1993) Purification and properties of a diisopropyl-fluorophosphatase from squid Todarodes-Pacificus-Steenstrup. *J. Biochem. Toxicol. 8*, 161–166.
7. Hill, C. M., Li, W. S., Cheng, T. C., DeFrank, J. J., and Raushel, F. M. (2001) Stereochemical specificity of organophosphorus acid anhydrolase toward p-nitrophenyl analogs of soman and sarin. *Bioorg. Chem. 29*, 27–35.
8. Harper, L. L., Mcdaniel, C. S., Miller, C. E., and Wild, J. R. (1988) Dissimilar plasmids isolated from *Pseudomonas diminuta* Mg and a *Flavobacterium* Sp (ATCC-27551) contain identical Opd genes. *Appl. Environ. Microbiol. 54*, 2586–2589.
9. Omburo, G. A., Kuo, J. M., Mullins, L. S., and Raushel, F. M. (1992) Characterization of the zinc binding site of bacterial phosphotriesterase. *J. Biol. Chem. 267*, 13278–13283.
10. Kolakowski, J. E., DeFrank, J. J., Harvey, S. P., Szafraniec, L. L., Beaudry, W. T., Lai, K. H., and Wild, J. R. (1997) Enzymatic hydrolysis of the chemical warfare agent VX and its neurotoxic analogues by organophosphorus hydrolase. *Biocatal. Biotransform. 15*, 297–312.
11. Benning, M. M., Shim, H., Raushel, F. M., and Holden, H. M. (2001) High resolution X-ray structures of different metal-substituted forms of phosphotriesterase from *Pseudomonas diminuta*. *Biochemistry 40*, 2712–2722.
12. Vanhooke, J. L., Benning, M. M., Raushel, F. M., and Holden, H. M. (1996) Three-dimensional structure of the zinc-containing phosphotriesterase with the bound substrate analog diethyl 4-methylbenzylphosphonate. *Biochemistry 35*, 6020–6025.
13. Chen-Goodspeed, M., Sogorb, M. A., Wu, F. Y., Hong, S. B., and Raushel, F. M. (2001) Structural determinants of the substrate and stereochemical specificity of phosphotriesterase. *Biochemistry 40*, 1325–1331.
14. Chen-Goodspeed, M., Sogorb, M. A., Wu, F. Y., and Raushel, F. M. (2001) Enhancement, relaxation, and reversal of the stereoselectivity for phosphotriesterase by rational evolution of active site residues. *Biochemistry 40*, 1332–1339.
15. Nowlan, C., Li, Y. C., Hermann, J. C., Evans, T., Carpenter, J., Ghanem, E., Shoichet, B. K., and Raushel, F. M. (2006) Resolution of chiral phosphate, phosphonate, and phosphinate esters by an enantioselective enzyme library. *J. Am. Chem. Soc. 128*, 15892–15902.
16. Li, W. S., Lum, K. T., Chen-Goodspeed, M., Sogorb, M. A., and Raushel, F. M. (2001) Stereoselective detoxification of chiral sarin and soman analogues by phosphotriesterase. *Bioorg. Med. Chem. 9*, 2083–2091.
17. Lum, K. T. (2004) Directed evolution of phosphotriesterase: Towards the efficient detoxification of sarin and soman. Ph.D. dissertation, Department of Toxicology, Texas A&M University, College Station, TX.
18. Hill, C. M., Li, W. S., Thoden, J. B., Holden, H. M., and Raushel, F. M. (2003) Enhanced degradation of chemical warfare agents through molecular engineering of the phosphotriesterase active site. *J. Am. Chem. Soc. 125*, 8990–8991.
19. Reeves, T. E., Wales, M. E., Grimsley, J. K., Li, P., Cerasoli, D. M., and Wild, J. R. (2008) Balancing the stability and the catalytic specificities of OP hydrolases with enhanced V-agent activities. *Protein Eng., Des. Sel. 21*, 405–412.
20. Li, Y., and Raushel, F. M. (2007) Differentiation of chiral phosphorus enantiomers by P-31 and H-1 NMR spectroscopy using amino acid derivatives as chemical solvating agents. *Tetrahedron: Asymmetry 18*, 1391–1397.
21. Yeung, D. T., Smith, J. R., Sweeney, R. E., Lenz, D. E., and Cerasoli, D. M. (2007) Direct detection of stereospecific soman hydrolysis by wild-type human serum paraoxonase. *FEBS J. 274*, 1183–1191.
22. Lum, K. T., Huebner, H. J., Li, Y. C., Phillips, T. D., and Raushel, F. M. (2003) Organophosphate nerve agent toxicity in *Hydra attenuata*. *Chem. Res. Toxicol. 16*, 953–957.